FEBS Letters 588 (2014) 2789–2793

journal homepage: www.FEBSLetters.org

A possible iron delivery function of the dinuclear iron center of HcgD in [Fe]-hydrogenase cofactor biosynthesis

Takashi Fujishiro [a], Ulrich Ermler [b], Seigo Shima [a,c,*]

[a] Max Planck Institute for Terrestrial Microbiology, Karl-von-Frisch-Straße 10, 35043 Marburg, Germany
[b] Max Planck Institute for Biophysics, Max-von-Laue-Straße 3, 60438 Frankfurt/Main, Germany
[c] PRESTO, Japan Science and Technology Agency (JST), Honcho, Kawaguchi, Saitama 332-0012, Japan

ARTICLE INFO

Article history:
Received 4 April 2014
Revised 16 May 2014
Accepted 27 May 2014
Available online 12 June 2014

Edited by Stuart Ferguson

Keywords:
Hydrogenase
Iron
Metal-cofactor biosynthesis
Metal-binding protein
X-ray crystallography
Nif3-like protein family

ABSTRACT

HcgD, a homolog of the ubiquitous Nif3-like protein family, is found in a gene cluster involved in the biosynthesis of the iron-guanylylpyridinol (FeGP) cofactor of [Fe]-hydrogenase. The presented crystal structure and biochemical analyses indicated that HcgD has a dinuclear iron-center, which provides a pronounced binding site for anionic ligands. HcgD contains a stronger and a weaker bound iron; the latter being removable by chelating reagents preferentially in the oxidized state. Therefore, we propose HcgD as an iron chaperone in FeGP cofactor biosynthesis, which might also stimulate investigations on the functionally unknown but physiologically important eukaryotic Nif3-like protein family members.

Structured summary of protein interactions:
HcgD and **HcgD** bind by X-ray crystallography (View interaction)

1. Introduction

[Fe]-hydrogenase is one of three classes of hydrogenases [1,2] and reversibly catalyzes the heterolytic cleavage of molecular hydrogen; the generated hydride is transferred to methenyl-tetrahydromethanompterin in a stereo-specific manner [3,4]. [Fe]-hydrogenase contains a mononuclear iron complex, the iron-guanylylpyridinol (FeGP) cofactor, which is essential for catalysis [5]. The iron of the FeGP cofactor is coordinated by two CO, one cysteine-S, one solvent, and one pyridinol nitrogen and one acyl-carbon of a pyridinol substituent [6–10]. Because of its unique structural features, as i.e. the organometallic iron-acyl bond and the highly substituted pyridinol, the biosynthesis of the FeGP cofactor is of great interest in chemistry and biology.

Seven highly conserved genes (*hcgA–G*) are adjacent to the *hmd* gene encoding [Fe]-hydrogenase. Their encoded proteins HcgA–G was postulated to be involved in FeGP-cofactor biosynthesis [4], which has been indirectly supported by recent genetic data from *Methanococcus maripaludis* [11]. HcgA was identified as a radical SAM enzyme by biochemical evidence, but its physiological function is not known [12]. We annotated HcgB as a guanylyltransferase catalyzing the conjugation of GMP and a pyridinol derivative to the guanylylpyridinol moiety of the FeGP cofactor [13]. Based on this result and stable-isotope labeling analysis [14], we have proposed that the guanylylpyridinol substrate is synthesized before formation of the iron center.

HcgD is a member of the Nif3 (NGG1p-interacting factor 3)-like protein family. The Nif3 protein was first identified in a yeast two-hybrid screening with the yeast dual regulator protein NGG1p [15]. A Nif3-like protein in mice is expressed throughout the embryonic development and might be involved in transcriptional regulation of neural differentiation. Its exact biochemical and physiological functions are, however, still obscure [16]. Nif3-like proteins might also be implicated in human diseases [17]. Crystal structures of Nif3-like proteins have revealed a dinuclear metal-binding site at the bottom of an interdomain cleft [18–22].

Here, we present the biochemical and crystal structure analyses of HcgD from *Methanocaldococcus jannaschii* (protein MJ0927) in different conditions. Based on the results we proposed a possible function of the protein in the biosynthesis of the FeGP cofactor.

Abbreviations: FeGP, iron-guanylylpyridinol; Hmd, H_2-forming methylene-tetrahydromethanopterin dehydrogenase; Hcg, Hmd co-occurring proteins; Nif3, NGG1p-interacting factor 3

* Corresponding author at: Max Planck Institute for Terrestrial Microbiology, Karl-von-Frisch-Straße 10, 35043 Marburg, Germany. Fax: +49 6421 178 109.
E-mail address: shima@mpi-marburg.mpg.de (S. Shima).

http://dx.doi.org/10.1016/j.febslet.2014.05.059
0014-5793/

2. Materials and methods

2.1. Preparation of HcgD

Escherichia coli BL21(DE3)Star cells that heterologously produce the His-tagged *M. jannaschii* HcgD protein (see Supplementary material for details) were re-suspended in a solution consisting of 50 mM potassium phosphate pH 7.0, 0.5 M KCl and 20 mM imidazole (buffer A) and disrupted by sonication. The supernatant was collected by centrifugation and loaded onto a Ni^{2+}-charged HiTrap chelating column (GE Healthcare) equilibrated with buffer A. The column was washed with buffer A, and proteins were eluted with a 20–500 mM linear gradient of imidazole in 50 mM potassium phosphate pH 7.0 and 0.5 M KCl. After desalting the protein fractions with 50 mM potassium phosphate, pH 7.0 and 0.3 M KCl, the protein solution was incubated with thrombin (10 units/mg HcgD protein) at 4 °C overnight to cleave the His-tag. The His-tag and thrombin were then removed by Ni^{2+}-charged HiTrap chelating and HiTrap Benzamidine FF (GE Healthcare) columns equilibrated with buffer A. Finally, the HcgD fractions were subjected to a HiPrep Sephacryl S-200 chromatographic step (GE Healthcare) using 50 mM potassium phosphate pH 7.0 and 0.3 M KCl for equilibration. The pure HcgD isolated was referred to as oxidized HcgD. To prepare reduced HcgD, oxidized HcgD was incubated with 10 mM sodium dithionite in a Coy chamber under a N_2/H_2 atmosphere (95%/5%) at room temperature for 3 h. Excess of sodium dithionite was removed with a desalting PD-10 column (GE Healthcare). EDTA-treated oxidized HcgD was prepared by incubation of oxidized HcgD with 0.25 M EDTA at 4 °C for more than 12 h and EDTA-treated, reduced HcgD by incubation of reduced HcgD with 0.25 M EDTA in a Coy chamber under a N_2/H_2 atmosphere (95%/5%) at room temperature for 12 h. After the incubation, excess EDTA, dithionite (if present), free and EDTA bound Fe ions were removed by a desalting PD-10 column.

2.2. UV–Vis spectroscopy, Fe quantification in a colorimetric assay and X-ray florecence scan

UV–Vis spectra of oxidized HcgD, reduced HcgD, and EDTA-treated HcgD were recorded on a Specord S 600 (Analytik Jena) with a quartz cell (0.3 cm cell path) at room temperature. Fe in HcgD was quantified using Ferene reagent [23] and Zn using *N*1-(7-nitro-2,1,3-benzoxadiazol-4-yl)-*N*1,*N*2,*N*2-tris(2-pyridinylmethyl)-1,2-ethanediamine (NBD-TPEA) [24]. X-ray fluorescence scans on HcgD crystals were performed at the Swiss-Light Source (Villigen, Switzerland).

2.3. Crystallization of HcgD

Oxidized HcgD (14 mg/mL) and reduced HcgD (18 mg/mL) stock solutions were prepared in 10 mM MOPS/KOH buffer pH 7.0. For crystallization, 1 μL oxidized HcgD (14 mg/mL) was mixed with 1 μL of a reservoir solution [35% (v/v) (±)-2-methyl-2,4-pentanediol, 0.2 M NaCl, 0.1 M Tris–HCl pH 7.0]. Reduced HcgD was crystallized by adding 1 μL reduced HcgD and 1 μL of a reservoir solution [10% (w/v) PEG8000, 0.2 M NaCl, 5 mM sodium dithionite, 0.1 M Na/K phosphate pH 6.2] under a N_2/H_2 atmosphere (95%/5%). Crystals of HcgD with citrate grew from 1 μL HcgD and 1 μL reservoir solution [10% (w/v) PEG4000, 10% (v/v) 2-propanol, 0.1 M sodium citrate pH 5.6]. For crystallization of reduced HcgD with citrate, 1 μL reduced HcgD was mixed with 1 μL of a reservoir solution [10% (w/v) PEG4000, 10% (v/v) 2-propanol, 5 mM sodium dithionite, 0.1 M sodium citrate pH 5.6] under a N_2/H_2 atmosphere (95%/5%). EDTA-treated HcgD was crystallized from a solution composed of 1 μL EDTA-treated HcgD (15 mg/mL) and 1 μL of reservoir solution [2.4 M ammonium sulfate, 0.1 M HEPES-NaOH pH 7.0]. Crystallization of EDTA-treated, reduced HcgD succeeded from 1 μL of EDTA-treated, reduced HcgD (18 mg/mL) and 1 μL reservoir solution [10% (w/v) PEG8000, 0.2 M NaCl, 5 mM sodium dithionite, 0.1 M Na/K phosphate pH 6.2] under a N_2/H_2 atmosphere (95%/5%). HcgD and pyridinol derivatives (5 mM 6-carboxymethyl-2-hydroxypyridine, 5 mM 3,6-dimethyl-2,4-dihydroxypyridine, or 1.25 mM iron-free FeGP cofactor prepared by photo-decomposition of extracted FeGP cofactor [10]) were co-crystallized under the same conditions as described above (Supplementary Fig. S1). All types of crystals were obtained using the sitting-drop vapor diffusion method at room temperature within two weeks.

2.4. X-ray data collection and refinement

The crystals were frozen under a cryo-stream of liquid nitrogen at 100 K. The crystals of reduced HcgD, oxidized and reduced HcgD with citrate, EDTA-treated HcgD in a reduced state were immersed into 33% (v/v) ethylene glycol-containing reservoir solutions for cryo-protection before cryo-freezing. Diffraction data were collected with a PILATUS 6 M detector at beamline X10SA of the Swiss-Light Source (Villigen, Switzerland) and processed using XDS [25]. All HcgD structures were solved by molecular replacement with BALBES [26], Molrep [27], or Phaser [28] based on the crystal structure of a conserved hypothetical protein from *Streptococcus pneumoniae* TIGR4 (PDB code: 2FYW) as a search model. Models were built and refined using COOT [29], REFMAC5 [30], and PHENIX [31]. In the final stage of refinement translation/libration/screw-rotation groups were introduced [32]. Structure validation was performed using COOT, PHENIX and PROCHECK [33]. The resulting structures were established at 2.5 Å (oxidized HcgD), 2.5 Å (reduced HcgD), 2.0 Å (HcgD with citrate), 2.0 Å (reduced HcgD with citrate), 2.8 Å (EDTA-treated HcgD), and 2.3 Å (EDTA-treated, reduced HcgD). Data collection and refinement statistics are summarized in Supplementary Table S1. All figures of proteins were depicted using PyMOL (Version 1.3r1, Schrödinger, LLC.). Model coordinates and structure factors were deposited in the Protein Data Bank under the following accession codes: 3WSD (oxidized HcgD), 3WSE (reduced HcgD), 3WSF (oxidized HcgD with citrate), 3WSG (reduced HcgD with citrate), 3WSH (EDTA-treated, oxidized HcgD), and 3WSI (EDTA-treated, reduced HcgD) (Supplementary Table S1).

3. Results and discussion

3.1. Characterization of the metal in HcgD

Oxidized HcgD from *M. jannaschii* heterologously produced and isolated from *E. coli* was slightly yellow, and the UV–Vis spectrum had two broad shoulder peaks at 320 and 360 nm (Fig. 1). The yellow color suggested the presence of iron, as found in the Nif3-related protein YbgI from *E. coli* [20], rather than zinc, present in the Nif3-related proteins YqfO from *Bacillus cereus* [18] and protein SA1388 from *Staphylococcus aureus* [19]. A colorimetric assay using Ferene reagent revealed absorption of a typical iron-Ferene complex at 593 nm with 1.7 ± 0.8 irons per monomer (data not shown). Moreover, X-ray fluorescence spectroscopic measurements on crystals of HcgD showed an anomalous signal at the iron absorption edge (not shown). No Zn was detected using NBD-TPEA. The UV–Vis spectrum of HcgD between 300 and 400 nm changed upon addition of dithionite; i.e. the peaks at 320 and 360 nm disappeared and a shoulder peak emerged at around 330 nm (Fig. 1), which suggested redox-active metal like iron ($Fe^{3+} \rightarrow Fe^{2+}$) bound to HcgD. These results indicated that HcgD most likely contains redox-active irons per monomer.

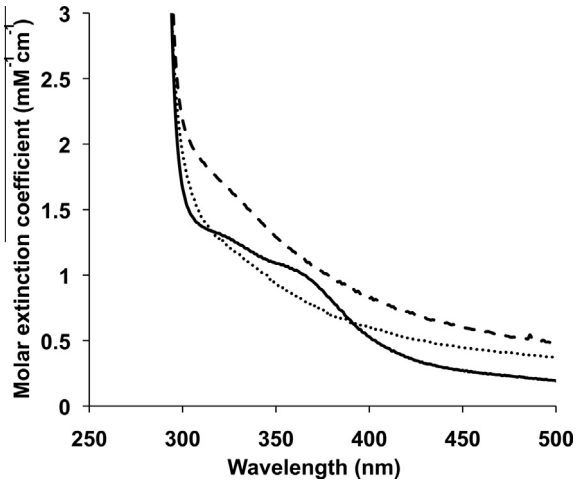

Fig. 1. UV–Vis spectra of oxidized HcgD (solid line), reduced HcgD (dashed line), and EDTA-treated oxidized HcgD (dotted line).

3.2. Crystal structures of oxidized and reduced HcgD

Oxidized HcgD and HcgD reduced with dithionite (2.5 mM final concentration after mixing 1 μL of a HcgD protein stock solution with 1 μL of a reservoir solution containing 5 mM dithionite in crystallization) were structurally characterized at 2.5 Å resolution (oxidized HcgD structure is shown in Fig. 2A). Both HcgD structures are virtually identical (Supplementary Fig. S2). HcgD, like other members of the Nif3-like protein family (Supplementary Fig. S3) [18–21], is organized as a hexameric toroid built up of a trimer of a compact dimer. The dimers are formed by a head-to-tail arrangement of two HcgD monomers each of them being composed of two similar interlinked α/β domains (Fig. 2A; Supplementary Fig. 2). The binuclear iron binding site is located at the inner side of the toroid at the bottom of a wide cleft formed between the two α/β domains of each HcgD monomer. The potential substrate binding site in front of the binuclear binding site is encircled by Pro72, His103, Thr104, Leu134, Leu176 and Tyr179 as well as His204 of the partner monomer which partly shields the active site from bulk solvent. In oxidized and reduced HcgD, the Fe1/Fe2 binding sites are occupied by two irons with an estimated occupancy of ca. 0.48/1.00 and 0.85/1.00, respectively. Independent of the redox state the two irons are 3.3–3.9 Å apart and ligated by the same residues that are strictly conserved in HcgD proteins from different species (Supplementary experimental procedures and Supplementary Fig. S4). His70-NE2 and Asp107-OD1 and/or -OD2 are coordinated to Fe1 and His71-NE2 and His221-NE2 to Fe2. The carboxyl group of the side chain of Glu225 is located between Fe1 and Fe2 to serve as a bridging ligand (Fig. 2B). In addition, further non-protein ligands connected to Fe2 were modeled as chloride and phosphate ions in the oxidized and reduced HcgD structures, respectively, according to the shape and height of the electron density (Fig. 2B). The anionic chloride and phosphate ions further interact with His103, via solvent molecules with Asn114ND2, Tyr179N, Ser177O and OG as well as with His204-NE2 of the partner monomer. This type of binding site for an anionic ligand has not been reported in structures, so far, available for Nif3-like proteins.

Recently, Kuan et al. independently published a preliminary X-ray crystallographic study on HcgD [22]; the crystallization conditions were different from our study. In January 2014 (just before the submission of our manuscript), the crystal structures of selenomethionine-labeled and native HcgD (PDB codes: 4IWM and 4IWG) were deposited in the RCSB Protein Data Bank, though the structural article has not been published and metals were not present in the structure. Therefore, the structure and properties of the iron site could not be compared.

3.3. Impact of the chelating reagents citrate and EDTA

According to the postulated reaction scheme of FeGP cofactor synthesis (Schick et al. [14], Fujishiro et al. [13]), HcgD is involved in the biosynthesis of the Fe center after forming a

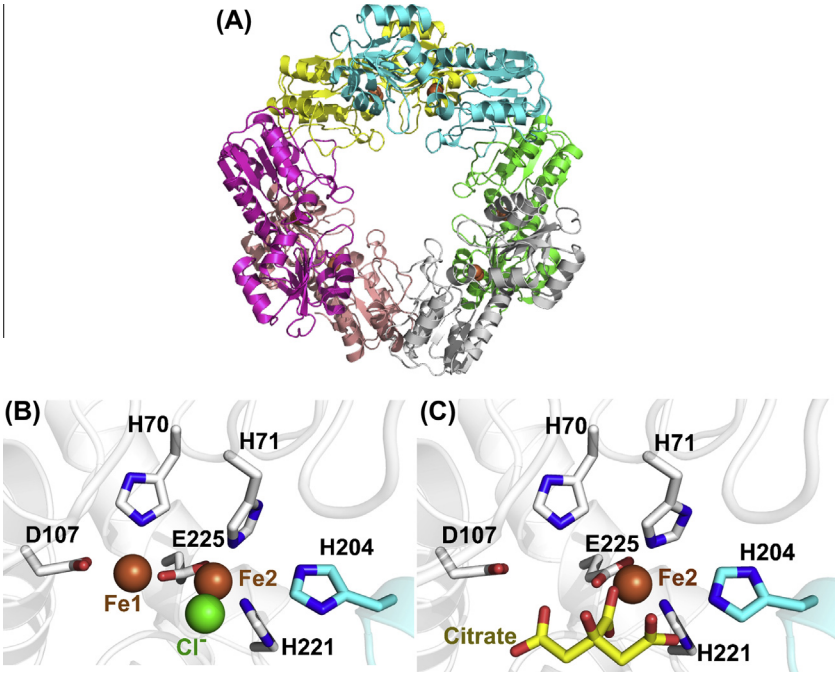

Fig. 2. (A) Homohexameric structure of oxidized HcgD. The compact dimers are drawn in red/lightred, gray/green and yellow/blue. (B) Iron-binding site of oxidized HcgD. The irons and the chloride are highlighted as brown and green spheres. Amino acids coordinating the irons, His204 and citrate are drawn as sticks. His204 (blue) protrudes from the partner subunit to the active site. (C) Iron-binding site of oxidized HcgD with citrate after removal of one iron.

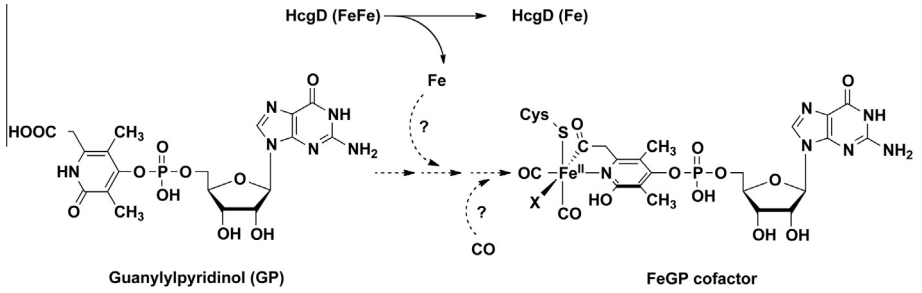

Fig. 3. A proposed function of HcgD in FeGP cofactor biosynthesis. The guanylylpyridinol precursor is converted by uncharacterized enzymes to the intact FeGP cofactor. We propose that one iron from HcgD could be delivered to a guanylylpridinol precursor. Enzyme reactions for the formation of the acyl- and CO-ligands and their ligation to the iron (arrows with dashed line and "?" symbols) are not characterized yet.

guanylylpyridinol precursor. Therefore, we tested the binding of several pyridinol compounds to the oxidized and reduced HcgD by co-crystallization experiments (for chemical structures of the pyridinol compounds, see Supplementary Fig. S1) but found no pyridinol compounds in the electron density of the corresponding crystal structures (data not shown). During structure analysis, we unexpectedly found that oxidized and reduced HcgD crystallized in the presence of 50 mM citrate (at a 1:1 protein/reservoir mixture in a crystallization drop) showed very weak electron density at the iron ion position of the Fe1 site and contained a citrate bound to the iron ion at the Fe2 site. Because of its very weak electron density and the limited resolution of the data, we did not model anything into the Fe1 site of oxidized (Fig. 2C) and reduced HcgD with citrate (data not shown). As the Fe1 ion appeared to be removed by citrate due to its chelating properties, the effects of other chelating reagents were also tested. Both oxidized and reduced HcgD were treated with 0.25 M EDTA in solution and subsequently free and iron ion bound EDTA were removed by desalting. Crystal structures of oxidized and reduced HcgD after EDTA treatment showed very weak electron density at the Fe1 sites as previously found in the crystal structures of HcgD incubated with citrate. On the other hand, Fe2 of EDTA-treated HcgD was not removed, however, ligated with anionic compounds (a sulfate and a phosphate in the oxidized and reduced HcgD, respectively). Removal of iron by the chelating agents was confirmed by UV–Vis spectroscopic and Fe analytical data. In the UV–Vis spectrum the height of the shoulder peaks between 300 and 400 nm was lower in the EDTA-treated than in the non-EDTA-treated oxidized HcgD (Fig. 1). Colorimetric iron analysis resulted in an iron content of 0.9 ± 0.3 irons per monomer for EDTA-treated, oxidized HcgD and 1.7 ± 0.8 irons per monomer for isolated HcgD. Interestingly, the Fe1 site of reduced HcgD appears to be less affected by EDTA. The EDTA-treated, reduced HcgD revealed an UV–Vis spectrum not significantly changed (data not shown) and an iron content (1.5 ± 0.4 irons per monomer) only moderately lower compared to the values of the isolated HcgD. Thus, crystal structure indicated that the affinity for iron was lower to the Fe1 than to the Fe2 site, and biochemical assays revealed that the affinity was lower in the oxidized than in the reduced state.

3.4. Arguments for the function of HcgD as an iron chaperone

Nif3 family proteins are characterized by their dinuclear metal centers composed of either iron or zinc. Our data clearly indicated that HcgD contains a dinuclear iron center. A second common feature of Nif3 proteins might be the binding site for an anionic ligand at the Fe2 site (or equivalent Zn site), which is occupied with either chloride, phosphate or citrate in HcgD as well as H_2O/OH^- ligands in the other Nif3 family structures [19,20]. The ligand-binding character at the metal clusters in Nif3 family members is distinct from those of other functionally known enzymes (e.g. iron-dependent ribonucleotide reductase and methane monooxygenase) [34], which prompts for a different function.

Biosynthesis of many metal-containing cofactors of enzymes requires metal-trafficking proteins [35], which most likely holds also true for FeGP cofactor maturation. According to sequence analysis HcgD is the only Hcg protein that potentially binds an iron rather than a Fe/S cluster [4], which makes it to an attractive candidate as an iron chaperone. The presented biochemical/structural data for HcgD revealed a stronger (Fe2) and a weaker (Fe1) binding site; the Fe1 site binds iron weaker under oxidized than under reduced conditions, which is compatible with a redox-state-dependent release process. A preferential and inducible release of one iron qualifies HcgD as an Fe chaperone (Fig. 3). The structural data further suggest that the potential Fe release from HcgD is linked with the binding of an ligand to Fe2. Residues forming the ligand binding site are strictly conserved within HcgD family. The physiological ligand for HcgD might be the guanylylpyridinol, which was identified as an intermediate in the FeGP cofactor biosynthesis [13]. This hypothesis could not be demonstrated by structural analysis of HcgD co-crystallized with guanylylpyridinol, but might be still possible as other maturation proteins might modulate HcgD and/or the guanylylpyridinol to promote iron transfer. The shallow pocket in front of the diiron center would provide sufficient space to bind a guanylylpyridinol derivative. Whether Fe1 is accepted by a guanylylpyridinol compound for further maturation or enzymatically equipped with CO ligands in the HcgD bound state and then further processed remains open. It has to be considered that the protein machinery recruited for the complex Fe center maturation process and the specific role of HgcD therein is still completely unclear.

4. Conclusion

The available data about HcgD are in agreement with a function as an iron chaperone that is involved in supplying an iron in the FeGP cofactor biosynthesis (Fig. 3). Stimulated by the described results, further biochemical studies are required to work out the specific role of HcgD in iron trafficking and Fe center maturation orchestrated by various maturation factors. Nif3-related proteins, widely distributed in the three domains of life, participate in vital physiological processes; however, the molecular functions of none of them are elucidated. Because of their high structural similarities, the metal-releasing and ligand-binding properties of HcgD might be common features of Nif3-related proteins and pave the path for further studies. Notably, human NIF3L1 [36] and mouse Nif3l1

[16] have been identified as components for neural differentiation. The neural differentiation in developing hippocampus is reported to be affected by perinatal iron deficiency [37].

Conflict of interest

The authors declare no conflicts of interest.

Acknowledgements

We thank Prof. Dr. Rolf Thauer for discussions and helpful suggestions; Prof. Dr. Hartmut Michel for continuous support; the staff of the PXII beamline at the Swiss-Light-Source, Villigen, and Ulrike Demmer for their help during data collection/X-ray structure analysis; and Dr. Haruka Tamura for construction of the HcgD expression system. We thank Prof. Dr. Xiaoming Liu for providing us a pyridinol compound. This work was supported by a Grant of the Max Planck Society to R.K. Thauer and a grant of the PRESTO program from the Japan Science and Technology Agency to S.S.

Appendix A. Supplementary data

Supplementary data associated with this article can be found, in the online version, at http://dx.doi.org/10.1016/j.febslet.2014.05.059.

References

[1] Fontecilla-Camps, J.C., Volbeda, A., Cavazza, C. and Nicolet, Y. (2007) Structure/function relationships of [NiFe]- and [FeFe]-hydrogenases. Chem. Rev. 107, 4273–4303.
[2] Vignais, P.M. and Billoud, B. (2007) Occurrence, classification, and biological function of hydrogenases: an overview. Chem. Rev. 107, 4206–4272.
[3] Shima, S. and Ermler, U. (2011) Structure and function of [Fe]-hydrogenase and its iron-guanylylpyridinol (FeGP) cofactor. Eur. J. Inorg. Chem. 2011, 963–972.
[4] Thauer, R.K., Kaster, A.K., Goenrich, M., Schick, M., Hiromoto, T. and Shima, S. (2010) Hydrogenases from methanogenic archaea, nickel, a novel cofactor, and H_2 storage. Annu. Rev. Biochem. 79, 507–536.
[5] Tamura, H., Salomone-Stagni, M., Fujishiro, T., Warkentin, E., Meyer-Klaucke, W., Ermler, U. and Shima, S. (2013) Crystal structures of [Fe]-hydrogenase in complex with inhibitory isocyanides: implications for the H_2-activation site. Angew. Chem. Int. Ed. 52, 9656–9659.
[6] Hiromoto, T. et al. (2009) The crystal structure of C176A mutated [Fe]-hydrogenase suggests an acyl-iron ligation in the active site iron complex. FEBS Lett. 583, 585–590.
[7] Hiromoto, T., Warkentin, E., Moll, J., Ermler, U. and Shima, S. (2009) The crystal structure of an [Fe]-hydrogenase-substrate complex reveals the framework for H_2 activation. Angew. Chem. Int. Ed. 48, 6457–6460.
[8] Shima, S. et al. (2008) The crystal structure of [Fe]-hydrogenase reveals the geometry of the active site. Science 321, 572–575.
[9] Shima, S., Schick, M., Kahnt, J., Ataka, K., Steinbach, K. and Linne, U. (2012) Evidence for acyl-iron ligation in the active site of [Fe]-hydrogenase provided by mass spectrometry and infrared spectroscopy. Dalton Trans. 41, 767–771.
[10] Lyon, E.J., Shima, S., Boecher, R., Thauer, R.K., Grevels, F.W., Bill, E., Roseboom, W. and Albracht, S.P.J. (2004) Carbon monoxide as an intrinsic ligand to iron in the active site of the iron-sulfur-cluster-free hydrogenase H_2-forming methylenetetrahydromethanopterin dehydrogenase as revealed by infrared spectroscopy. J. Am. Chem. Soc. 126, 14239–14248.
[11] Lie, T.J., Costa, K.C., Pak, D., Sakesan, V. and Leigh, J.A. (2013) Phenotypic evidence that the function of the [Fe]-hydrogenase Hmd in *Methanococcus maripaludis* requires seven hcg (hmd co-occurring genes) but not hmdII. FEMS Microbiol. Lett. 343, 156–160.
[12] McGlynn, S.E., Boyd, E.S., Shepard, E.M., Lange, R.K., Gerlach, R., Broderick, J.B. and Peters, J.W. (2010) Identification and characterization of a novel member of the radical AdoMet enzyme superfamily and implications for the biosynthesis of the Hmd hydrogenase active site cofactor. J. Bacteriol. 192, 595–598.
[13] Fujishiro, T., Tamura, H., Schick, M., Kahnt, J., Xiulan, X., Ermler, U. and Shima, S. (2013) Identification of the HcgB enzyme in [Fe]-hydrogenase-cofactor biosynthesis. Angew. Chem. Int. Ed. 52, 12555–12558.
[14] Schick, M., Xie, X.L., Ataka, K., Kahnt, J., Linne, U. and Shima, S. (2012) Biosynthesis of the iron-guanylylpyridinol cofactor of [Fe]-hydrogenase in methanogenic archaea as elucidated by stable-isotope labeling. J. Am. Chem. Soc. 134, 3271–3280.
[15] Martens, J.A., Genereaux, J., Saleh, A. and Brandl, C.J. (1996) Transcriptional activation by yeast PDR1p is inhibited by its association with NGG1p/ADA3p. J. Biol. Chem. 271, 15884–15890.
[16] Akiyama, H., Fujisawa, N., Tashiro, Y., Takanabe, N., Sugiyama, A. and Tashiro, F. (2003) The role of transcriptional corepressor Nif3l1 in early stage of neural differentiation via cooperation with Trip15/CSN2. J. Biol. Chem. 278, 10752–10762.
[17] Galperin, M.Y. and Koonin, E.V. (2004) 'Conserved hypothetical' proteins: prioritization of targets for experimental study. Nucleic Acids Res. 32, 5452–5463.
[18] Godsey, M.H., Minasov, G., Shuvalova, L., Brunzelle, J.S., Vorontsov, I.I., Collart, F.R. and Anderson, W.F. (2007) The 2.2 Å resolution crystal structure of *Bacillus cereus* Nif3-family protein YqfO reveals a conserved dimetal-binding motif and a regulatory domain. Protein Sci. 16, 1285–1293.
[19] Saikatendu, K.S., Zhang, X.J., Kinch, L., Leybourne, M., Grishin, N.V. and Zhang, H. (2006) Structure of a conserved hypothetical protein SA1388 from S. aureus reveals a capped hexameric toroid with two PII domain lids and a dinuclear metal center. BMC Struct. Biol. 6, 27.
[20] Ladner, J.E., Obmolova, G., Teplyakov, A., Howard, A.J., Khil, P.P., Camerini-Otero, R.D. and Gilliland, G.L. (2003) Crystal structure of *Escherichia coli* protein ybgI, a toroidal structure with a dinuclear metal site. BMC Struct. Biol. 3, 7.
[21] Tomoike, F., Wakamatsu, T., Nakagawa, N., Kuramitsu, S. and Masui, R. (2009) Crystal structure of the conserved hypothetical protein TTHA 1606 from *Thermus thermophilus* HB8. Proteins 76, 244–248.
[22] Kuan, S.M., Chen, H.C., Huang, C.H., Chang, C.H., Chen, S.C., Yang, C.S. and Chen, Y. (2013) Crystallization and preliminary X-ray diffraction analysis of the Nif3-family protein MJ0927 from *Methanocaldococcus jannaschii*. Acta Crystallogr. F 69, 80–82.
[23] Hennessy, D.J., Reid, G.R., Smith, F.E. and Thompson, S.L. (1984) Ferene – a new spectrophotometric reagent for iron. Can. J. Chem. 62, 721–724.
[24] Qian, F., Zhang, C.L., Zhang, Y.M., He, W.J., Gao, X., Hu, P. and Guo, Z.J. (2009) Visible light excitable Zn^{2+} fluorescent sensor derived from an intramolecular charge transfer fluorophore and its in vitro and in vivo application. J. Am. Chem. Soc. 131, 1460–1468.
[25] Kabsch, W. (2010) XDS. Acta Crystallogr. D 66, 125–132.
[26] Long, F., Vagin, A.A., Young, P. and Murshudov, G.N. (2008) BALBES: a molecular-replacement pipeline. Acta Crystallogr. D 64, 125–132.
[27] Vagin, A. and Teplyakov, A. (1997) MOLREP: an automated program for molecular replacement. J. Appl. Crystallogr. 30, 1022–1025.
[28] Mccoy, A.J., Grosse-Kunstleve, R.W., Adams, P.D., Winn, M.D., Storoni, L.C. and Read, R.J. (2007) Phaser crystallographic software. J. Appl. Crystallogr. 40, 658–674.
[29] Emsley, P. and Cowtan, K. (2004) Coot: model-building tools for molecular graphics. Acta Crystallogr. D 60, 2126–2132.
[30] Murshudov, G.N., Vagin, A.A. and Dodson, E.J. (1997) Refinement of macromolecular structures by the maximum-likelihood method. Acta Crystallogr. D 53, 240–255.
[31] Afonine, P.V., Mustyakimov, M., Grosse-Kunstleve, R.W., Moriarty, N.W., Langan, P. and Adams, P.D. (2010) Joint X-ray and neutron refinement with phenix.refine. Acta Crystallogr. D 66, 1153–1163.
[32] Winn, M.D., Isupov, M.N. and Murshudov, G.N. (2001) Use of TLS parameters to model anisotropic displacements in macromolecular refinement. Acta Crystallogr. D 57, 122–133.
[33] Laskowski, R.A., Macarthur, M.W., Moss, D.S. and Thornton, J.M. (1993) Procheck – a program to check the stereochemical quality of protein structures. J. Appl. Crystallogr. 26, 283–291.
[34] Wallar, B.J. and Lipscomb, J.D. (1996) Dioxygen activation by enzymes containing binuclear non-heme iron clusters. Chem. Rev. 96, 2625–2658.
[35] Waldron, K.J. and Robinson, N.J. (2009) How do bacterial cells ensure that metalloproteins get the correct metal? Nat. Rev. Microbiol. 7, 25–35.
[36] Tascou, S., Kang, T.W., Trappe, R., Engel, W. and Burfeind, P. (2003) Identification and characterization of NIF3L1 BP1, a novel cytoplasmic interaction partner of the NIF3L1 protein. Biochem. Biophys. Res. Commun. 309, 440–448.
[37] Tran, P.V., Carlson, E.S., Fretham, S.J.B. and Georgieff, M.K. (2008) Early-life iron deficiency anemia alters neurotrophic factor expression and hippocampal neuron differentiation in male rats. J. Nutr. 138, 2495–2501.